

MAGNETIC FIELD DERIVATIVES  
IN  
GEOPHYSICAL INTERPRETATION

by

Sheldon Breiner

Submitted to Professor Joshua L. Soske,  
Department of Geophysics, Stanford University  
fulfilling the requirements on original re-  
search for the degree of Master of Science

March 10, 1962

*Sheldon Breiner*

Introduction

The variations in the earth's magnetic field have served as the basis for the oldest presently used method of geophysical exploration. As early as 1643 the Swedish mining compass was used as a relatively crude but effective measure of the increases of intensity in the vicinity of an ore body.

The means with which the field or its variations were measured grew progressively more complex through such instruments as the dip needle, Hotchkiss super dip and the Schmidt-type magnetic field balance. The past decade has seen the replacement of these mechanical systems by sophisticated electronic instruments, namely, the fluxgate and proton precession magnetometer.

The great volume of magnetic data acquired by these electronic airborne units promoted the development of new methods and aids to interpretation and data handling. The most accepted of these methods are those involving computed derivative maps as suggested in the literature by Evjen (1936), Peters (1949), Henderson and Zietz (1949), Elkins (1951), Rosenbach (1953), and Henderson (1960).

These maps together with the original total intensity maps are utilized for qualitative interpretation only. 'Quantitative' use of magnetic contour maps was introduced by Vacquier et al in 1951 for the purpose of making depth determinations.

This method does not lend itself to rigorous mathematical analysis yet it provides a means for determining the depth to basement to approximately 10 or 20%. (Henderson and Zietz, 1955, p. 316)

At the time of this writing, however, an airborne magnetometer has been introduced that again requires the development of newer techniques of interpretation. The instrument is the rubidium vapor magnetometer whose basic sensitivity is approximately 0.01 gamma or about 100 times the sensitivity of the best previous magnetometers. To utilize this sensitivity in light of the advances already made in interpretation, the magnetometer was designed as a derivative measuring instrument, or gradiometer. The quality and variety of information now available in the magnetometer and gradiometer warrants the study of new methods of analysis. It was on this basis that the following investigation was performed on derivative maps and their aid to interpretation.

## Part II

### Derivative Maps

#### 1. A Qualitative Comparison with Total Intensity Maps

A derivative map in appearance is very much like its corresponding total intensity map. The differences that exist however, no matter how small, are often very significant in the interpretation of the subsurface structure.

The most significant feature of the derivative map is the presence of anomalous peaks and depressions not apparent on the total intensity maps. The slopes of the total intensity anomalies are exaggerated on the derivative map while the very slightly dipping portions are smoothed. As a consequence, slight irregular changes in intensity on the flanks of an anomaly which are caused by the superposition of more than one disturbance are effectively isolated. The amount of resolution is greater as the degree of derivative increases.

It is interesting to observe in various ways the mechanism responsible for this property. Analytically, the increased resolution is largely the result of the greater fall-off of the derivative with respect to its total intensity functions. In the very general case of the intensity from a point source, for example

$$H = \frac{K}{r^2}$$

where K is constant representing susceptibility, volume, etc..

The first derivative would then be  $\frac{\partial H}{\partial r} = -\frac{K}{r^3}$ .

Thus, as a consequence of the higher rate of fall-off, the derivative is more sensitive to a change in the radius to the disturbance. Two sources having two radii are therefore easily seen as a change in the derivative. The higher rate of fall-off, then, accounts for the increased resolution and related phenomenon mentioned above.

Graphically, the curves in Figure 1 represent the intensity at five depths. The information on the curves was transposed to the form of intensity,  $H_1$ , as a function of depth,  $z$ , for various points,  $x$ , on the profile line.

To a good approximation,

$$\begin{aligned} \left. \frac{\partial H}{\partial z} \right|_{x_1} &= \text{slope of } \left[ H|_{x_1} = f(z) \right]_{x_1} \\ &= \tan \theta \quad \text{where } \theta = \arctan \left( \left. \frac{H}{z} \right|_{x_1} \right) \end{aligned}$$

At  $z = z_0$ ,  $\frac{\partial H}{\partial z}$  was replotted as a function of  $x^1$ . In this case it is the tangent function that causes the steepening, the decrease of horizontal displacement of the peak, and the quick return to 'zero' of the curve  $\frac{\partial H}{\partial z} = f(x)$  when compared to  $H = g(x)$ .

<sup>1</sup> The graphical plotting and converting of  $H = g(x)$  to  $\frac{\partial H}{\partial z} = f(z)$  and back to  $\frac{\partial H}{\partial z} = h(x)$  was done without regard to scale or units; hence, the resulting plot is strictly qualitative

A second important difference between total intensity and derivative maps is the shift of the anomaly peaks and depressions. The peaks of the first derivative anomalies are shifted about halfway between the total intensity peak and projection of the anomalous disturbance peak on the plane of the map. Similarly, from the first vertical derivative to the second vertical derivative, the peak of the latter is then almost coincidental with the center of the anomalous disturbance itself <sup>2</sup>. See Figure 1.

A third but somewhat trivial difference is the change of units from one map to another, from intensity to intensity/distance. Moreover, if one treats the first derivative as a scalar potential and the second derivative as the first derivative of the potential, i.e., letting

$$\frac{\partial H}{\partial z} = \mathcal{X} \quad \text{and} \quad \frac{\partial^2 H}{\partial z^2} = \frac{\partial \mathcal{X}}{\partial z} ,$$

then it follows that for all the properties enumerated, the second derivative possesses the same properties and increases of resolution over the first derivative as does the first derivative over the total intensity.

<sup>2</sup> The amount of shift is also a function of inclination. The fractions given here are for middle latitude inclinations.

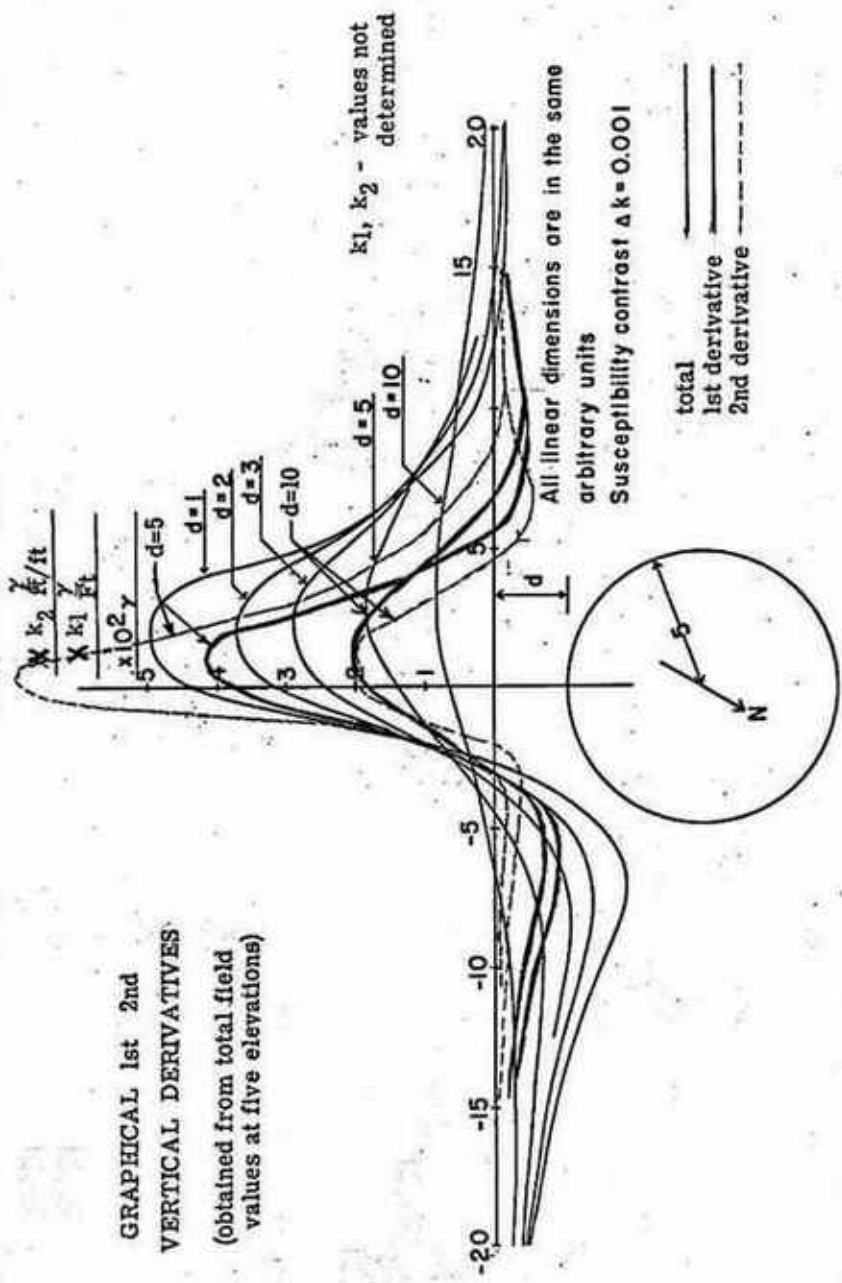


Figure 1

## 2. Computed Derivatives

Computed derivative maps are utilized by most geophysicists as an aid to interpretation. A variety of types of maps have been proposed in the literature each claiming to be superior in some aspect of interpretation. Commonly included in this variety are those known as residual, downward, and upward continuation maps and, of course, first and second and even fourth vertical derivative maps. Their utility is purely qualitative, the objective being greater resolution of the individual anomalies. This is accomplished by the process described in Part II, 1.

Even more numerous than the types of maps are the mathematical formulations derived by the authors mentioned above. It is generally agreed that no one method of computing a derivative map offers a much more accurate and informative picture than any other, though the most frequently used are second derivative maps<sup>3</sup>. All of the computed derivative maps originate from a map of a "potential" field which, taken by itself, does not owe its origin to a single, unique source. "The ambiguity arises from the fact that, given the distribution of a gravity, magnetic, or electric potential function over a surface... , it is not possible to derive a single unique distribution of mass, magnetization, or electric charge which will account for that field." ( Nettleton, 1954, p. 2.).

<sup>3</sup> They are used mostly because the most straightforward method of obtaining a derivative from a distribution of a potential over a plane involves the use of Laplace's equation,

$$\frac{\partial^2 H}{\partial x^2} + \frac{\partial^2 H}{\partial y^2} + \frac{\partial^2 H}{\partial z^2} = 0 .$$

A rather comprehensive formula was developed by Henderson (1960) which facilitates the computation of practically all the types of derivative maps mentioned earlier. The formula was programmed on various computers thereby eliminating the task of calculation and permitting a larger and more accurate sampling of the field values. This program was used by the writer to obtain computed maps and profiles (included in report) as a basis for comparison with measured profiles and subsequent development of derivative interpretation. It is not the writer's intent, however, to include here a discussion of the theory or virtues of the derivative formula except to say that it is one which involves the average of values on many circles of different radii.

Portions of a total intensity aeromagnetic map for which the derivatives were computed are shown in Figure 2. Superimposed over these anomalies are profile lines and a small segment of the grid used to sample the field values. The grid interval was chosen for both empirical and convenient reasons to be 3200 feet. The total intensity and computed first and second derivatives appear in Figures 3, 4, 5.

Probably the most critical step in computing a derivative map is the choice of the grid interval which determines the radii of the circles and, therefore, the points from which the field is sampled. It is an empirical choice but one which is generally found to be a controlling factor in both the values and character of the derivative map. (Peters, 1949; Nettleton, 1954). In Figure 6, for example, various profiles are shown

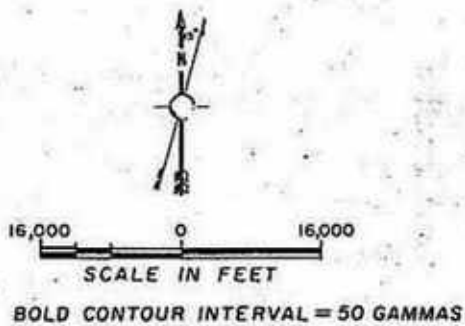
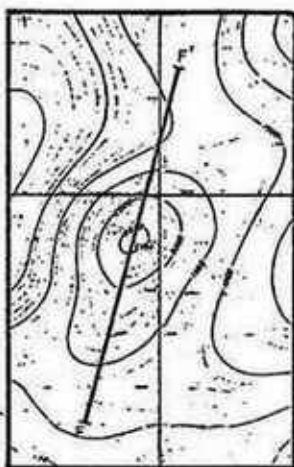
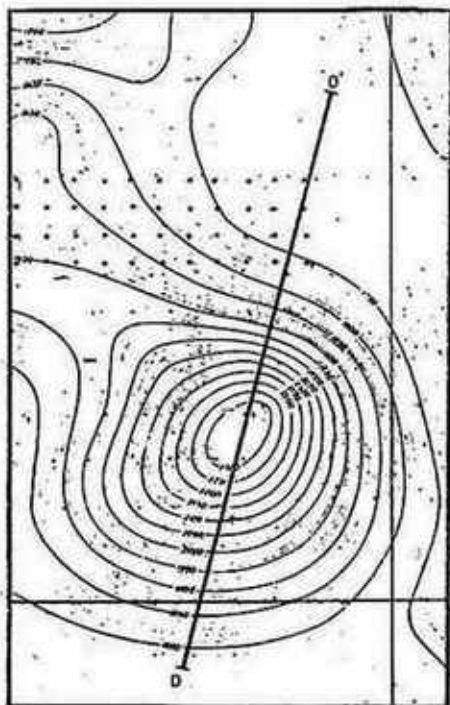
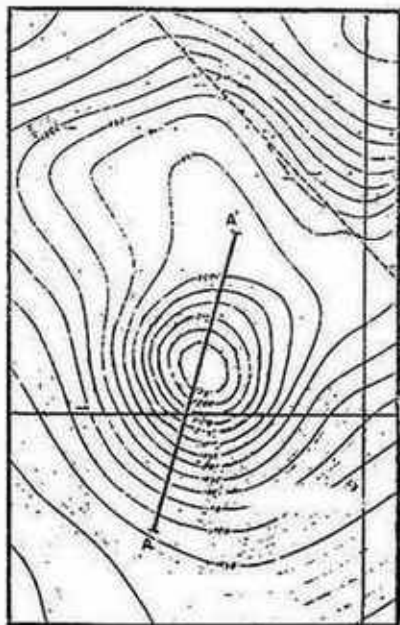


FIGURE 2. PROFILE LINES ON TOTAL INTENSITY MAP.

# Anomaly A

Computed Profiles

8750 feet

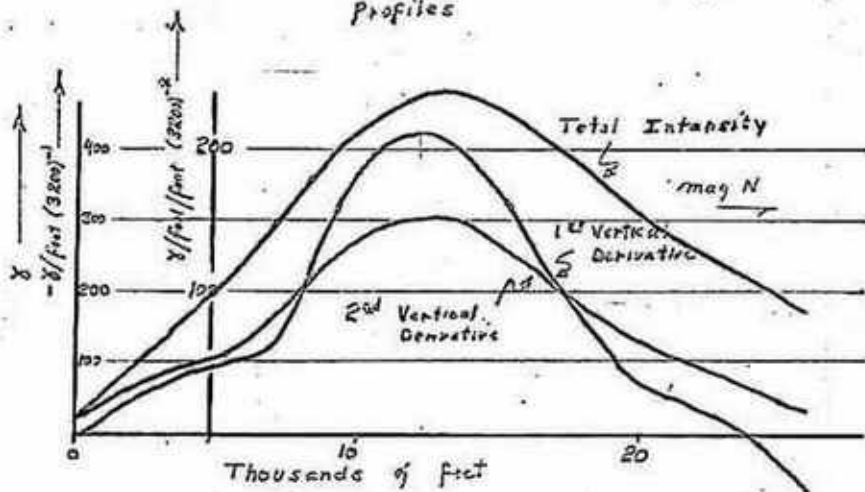


Figure 3.

# Anomaly F

Computed Profiles

7000 feet

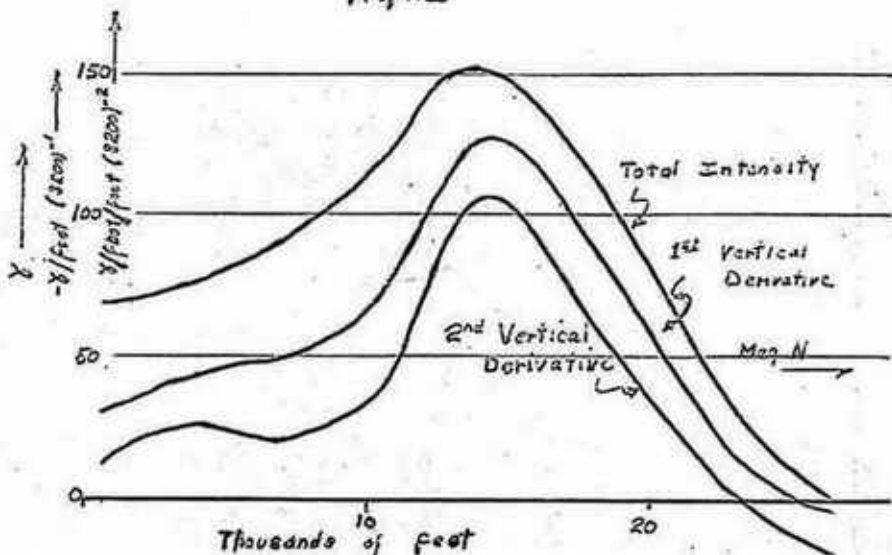


Figure 4.

# Anomaly D Computed Profiles

7000 feet

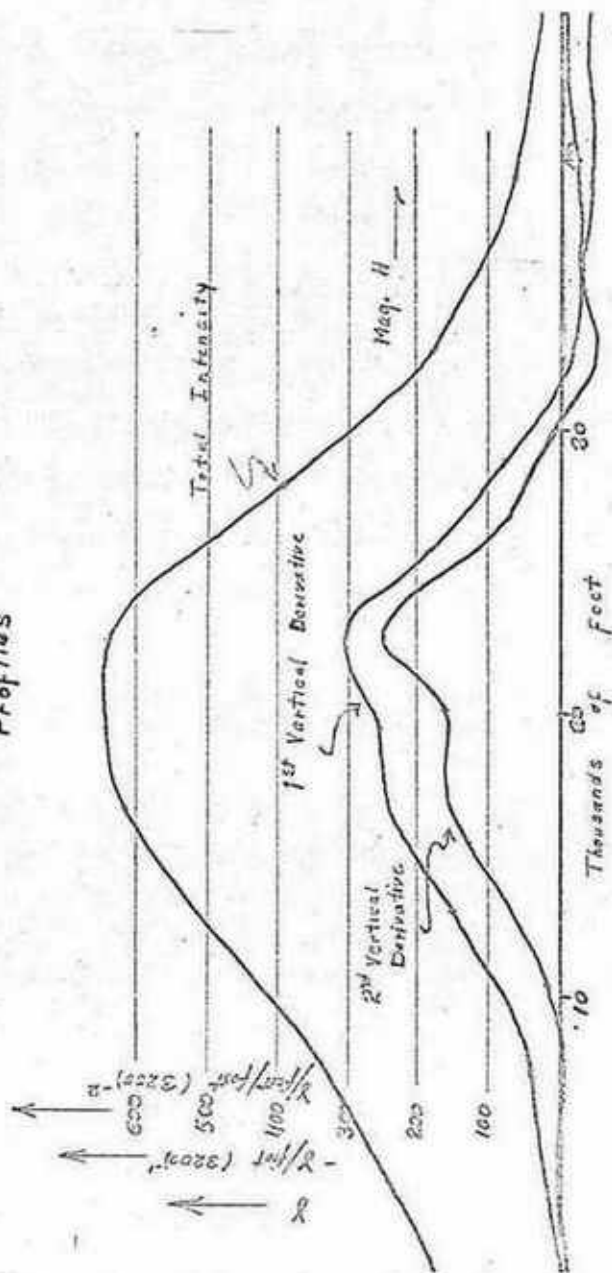
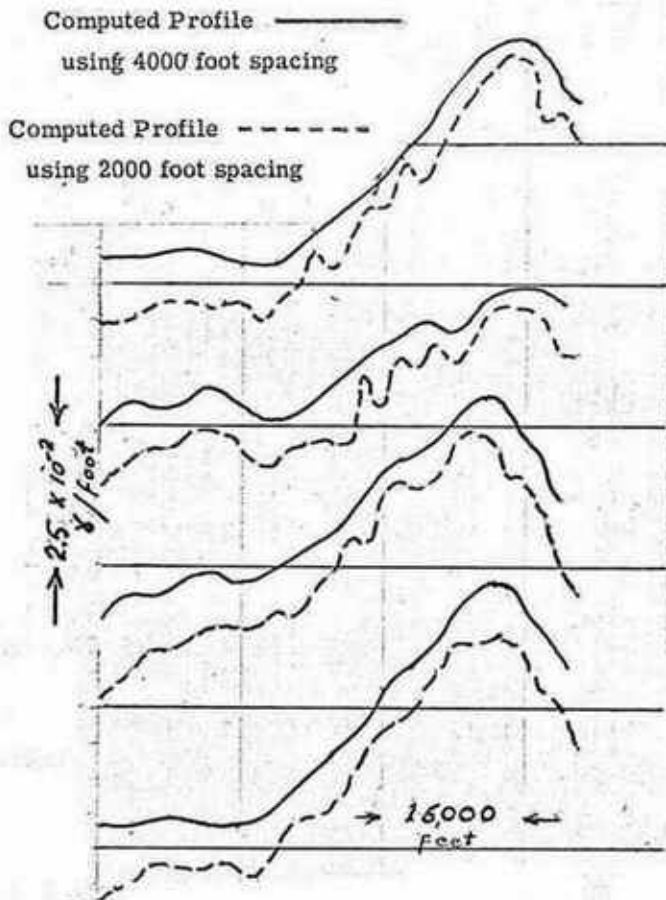


Figure 5.



COMPARISON OF COMPUTED DERIVATIVE PROFILES  
USING DIFFERENT GRID INTERVALS

Figure 6.

from a second vertical derivative map computed on the basis of two different size grids, one about equal to the average depth to basement and the other about one half that value. There is a decided difference in both the amplitude and oscillations of the anomaly derivatives, though the location and average slope of the major anomaly derivatives remain generally unchanged.

Other factors which limit the accuracy of derivative maps are a) the inaccuracy of chosen field data due to errors in contouring the total intensity map and errors in interpolating for the grid values, b) the approximations and theory used in the particular method of calculation (Trejo, 1954; Dean, 1958), and c) the previously mentioned non-unique solution from a plane of potential values.

### 3. The Measurement of the Derivative

As part of the development program referred to in the introduction, the gradiometer and magnetometer were flown over an area for which an aeromagnetic map (Figure 2), was available. This provided the rare opportunity to obtain and compare the computed derivative profiles with those actually measured.

With a view to examining the justification of measuring derivatives with the gradiometer, one must first understand the nature of the measurement and the derivative approximations. The gradiometer is merely a system which measures the difference between the intensity at two magnetometers which, in the case of the rubidium vapor instruments, measure total intensity. Since the gradient which is to be measured is vertical the magnetometers are, of course, displaced vertically.

The numerical approximation for the gradient or first derivative is

$$\left. \frac{\partial F(z)}{\partial r} \right|_{1.5} \approx \frac{F(2) - F(1)}{r_1}$$

where  $F(z)$  is the magnetic intensity at  $z$ , and  $r_1$  is distance between  $z = 1$  and  $z = 2$ .

The second derivative, similarly, can be expressed as

$$\frac{\partial^2 [F(z)]}{\partial r^2} \Big|_1 \approx \frac{\partial [F(0.5)]}{\partial r} - \frac{\partial [F(1.5)]}{\partial r}$$

$r_{2.5}$

$$\approx \frac{F(0) - F(1)}{r_1} - \frac{F(1) - F(2)}{r_2}$$

$r_{2.5}$

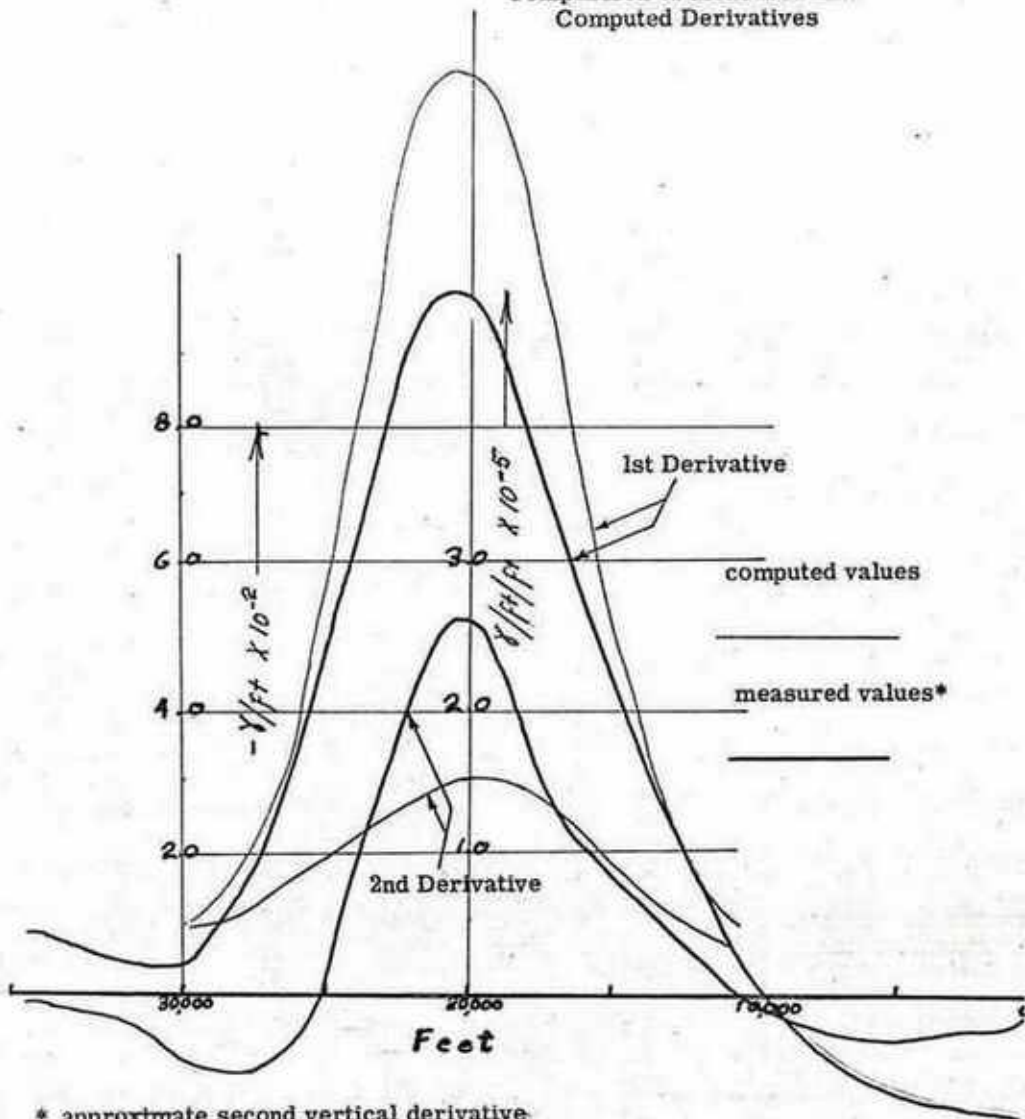
A more rigorous analysis of this justification in terms of

$$\frac{\partial H}{\partial z} = \frac{\Delta H}{\Delta z} \quad \text{is given in the Appendix at the close of the paper}$$

On this basis the first derivative or vertical gradient was measured on the profile lines of Figure 2. The measured derivative profiles are in Figures 7,8,9.

#### 4. Comparison of Computed and Measured Derivative Profiles

The comparisons of the derivatives are in Figures 7, 8,9. The second derivative was obtained for anomaly A by utilizing the information from two flights at different elevations in the same manner that the intensity from each magnetometer was used. Note the agreement in amplitude, (See Figures 8 & 9) and general character. Note also that the small anomalies that appear on the lower flanks of the computed anomalies agree with those on the measured profiles.

Comparison of Measured and  
Computed Derivatives

\* approximate second vertical derivative  
(difference of two 1st vertical derivatives divided by  
distance between)

average first vertical derivative  
(from two vertical derivatives at 9700' and 7700')

Figure 7.

COMPARISON OF MEASURED AND COMPUTED PROFILES

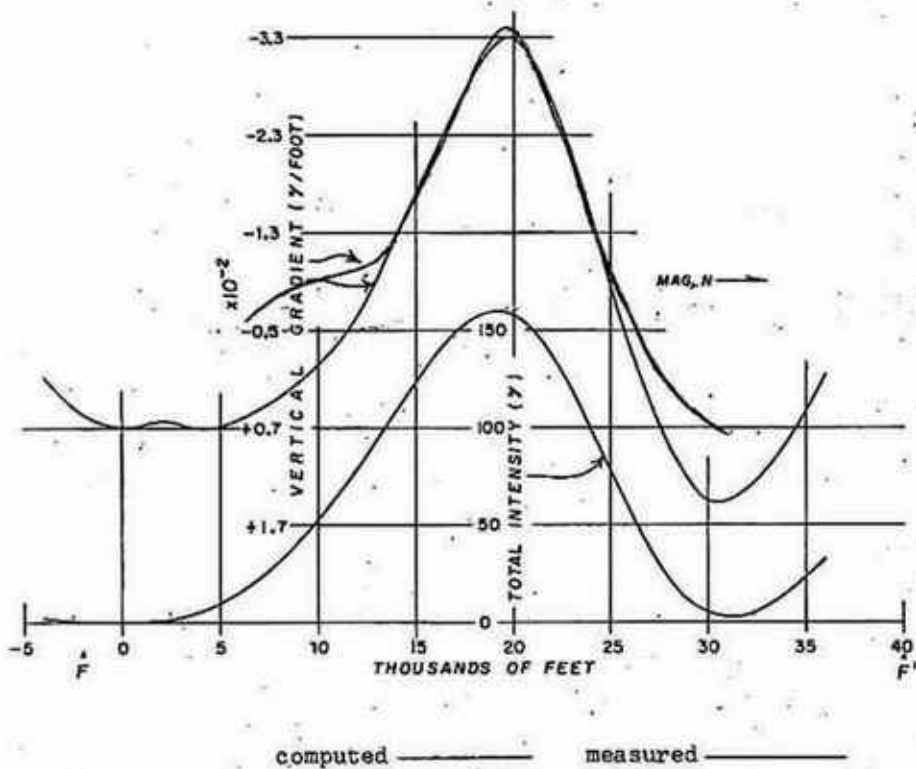


Figure 8.

COMPARISON OF MEASURED

AND

COMPUTED PROFILES

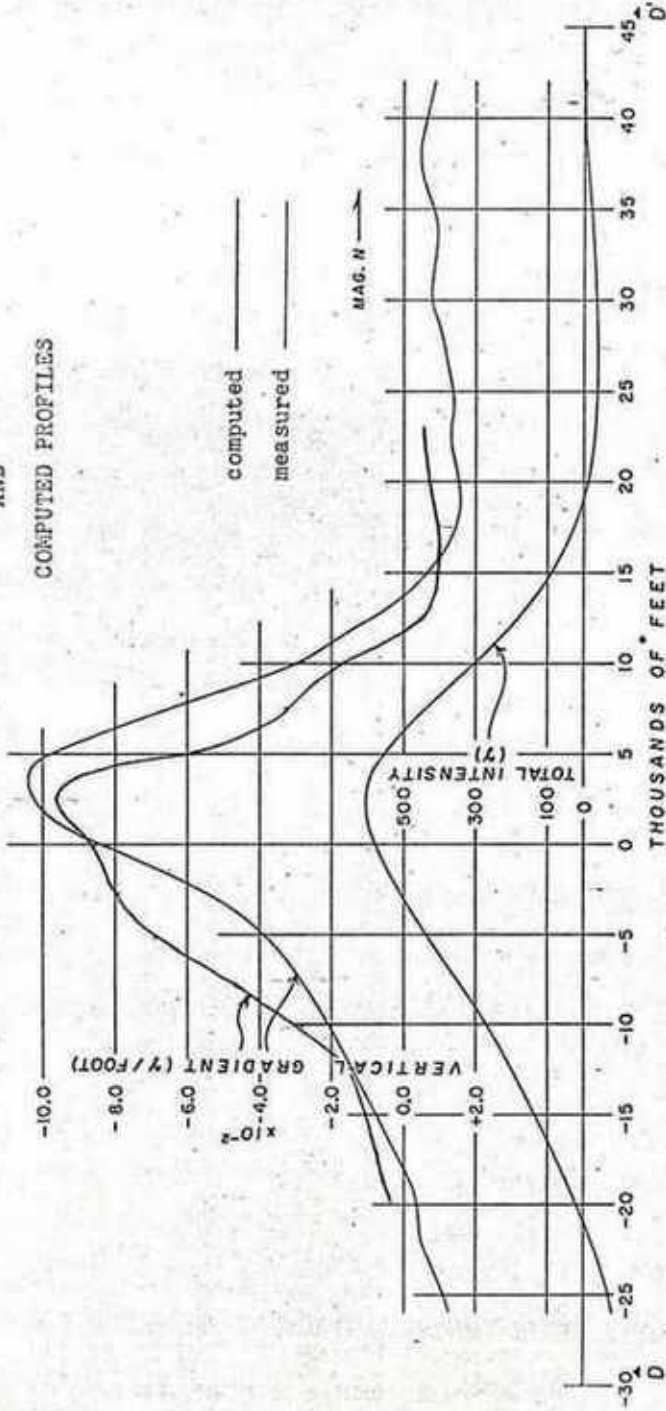


Figure 9.

Quantitative Application of Derivatives

## 1. Application of Derivatives to Basement Depth Determination

The investigation of the use of measured derivative information was directed largely towards the familiar problem of determining depth to basement from aerosurvey flight lines. The following represents suggestions on various procedures attempting to solve this problem.

The total magnetic field over the surface of the earth varies both in magnitude and direction in the vicinity of local natural disturbances. These disturbances are geologic in nature and owe their origin to intrusions, basement differentiations, or structures in the basement and sediments. The disturbance, or anomalous field, is caused by contrasts in the susceptibility in adjacent masses.

Exploration magnetometers, i.e., the rubidium vapor, proton precession, and the fluxgate instruments, for all practical purposes, measure the magnitude of the total field. This is particularly true in the case of smaller anomalies, e.g., 100-200 gammas.

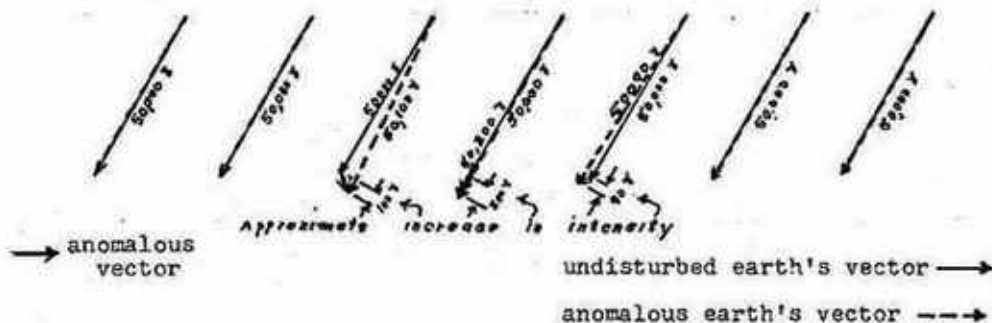


Figure 10.

It can be seen from Figure 10 that the change in the magnitude of the total field is essentially the component of the anomalous vector in the direction of the undisturbed earth's field.

These disturbances have at times been described as points, dipoles, lines of poles, lines of dipoles, and various prisms and bodies of revolution. If the magnetic field can be described by a mathematically homogeneous function, say,  $H(x,y,z)$ , it will satisfy Euler's Theorem on Homogeneous Functions,

$$(1) \frac{\partial [H(x,y,z)]}{\partial x} x + \frac{\partial [H(x,y,z)]}{\partial y} y + \frac{\partial [H(x,y,z)]}{\partial z} z = nH(x,y,z)$$

where  $n$  is the degree of homogeneity of the function  $H$  and a measure of the rate of fall-off with distance of magnetic intensity<sup>4</sup>. The origin of the coordinate system is the center of the anomalous magnetic disturbance where  $z$  is vertical and  $x$  and  $y$  are horizontal with  $x$  in the profile direction.

The values of  $H$  and  $\frac{\partial H}{\partial z}$  are obtained directly from the curves, and  $\frac{\partial H}{\partial x}$  is obtained from the plot of  $H$  vs  $x$ . The second term,  $y \frac{\partial H}{\partial y}$  is zero where the profile line is either over the anomaly ( $y=0$ ), or where the profile direction is perpendicular to the contour lines of the total intensity map, ( $\frac{\partial H}{\partial y}=0$ ).

At the peak of the total intensity anomaly

$$\frac{\partial H}{\partial x} = \frac{\partial H}{\partial y} = 0,$$

<sup>4</sup> In the case of a point source, for example, where  $H = \frac{K}{r^2}$ ,  $n = -2$ .

For a dipole,  $n = -3$ .

and Euler's theorem can be expressed in the simpler form

$$(2) \quad z = n \frac{H_p}{\left. \frac{\partial H}{\partial z} \right|_p}$$

This form of the theorem will also hold at a point on the profile line where, as before,  $\frac{\partial H}{\partial y} = 0$  (or  $y=0$ ) but where  $x=0$ . Thus, the point on the profile not on the peak where

$$(3) \quad z = n \frac{H_o}{\left. \frac{\partial H}{\partial z} \right|_o} = n \frac{H_p}{\left. \frac{\partial H}{\partial z} \right|_p}$$

is the point from which  $x$  is measured, and this point is immediately over the source.

Euler's theorem, as it is here used, then is

$$x \frac{\partial H}{\partial x} + z \frac{\partial H}{\partial z} = nH$$

where the unknowns are  $z$  and  $n$ . To solve for them, the theorem is evaluated at various values of  $x$ . The resulting straight line equations of  $z$  and  $n$  are plotted, and their intersection represents the solution for  $z$  and  $n$ .

Many points on the profile meet the conditions necessary to solve for the unknowns, a fact which is used in obtaining difference values rather than the more difficult-to-determine absolute values of the derivative and of the field.

We have

$$(4) \quad \left. \frac{\partial H}{\partial x} \right|_2 x_2 + \left. \frac{\partial H}{\partial z} \right|_2 z = n H_2$$

$$(5) \quad \left. \frac{\partial H}{\partial x} \right|_3 x_3 + \left. \frac{\partial H}{\partial z} \right|_3 z = n H_2 \quad \text{and}$$

$$(6) \quad \left. \frac{\partial H}{\partial x} \right|_2 x_2 - \left. \frac{\partial H}{\partial x} \right|_3 x_3 + \left[ \left. \frac{\partial H}{\partial z} \right|_2 - \left. \frac{\partial H}{\partial z} \right|_3 \right] z = n [H_2 - H_3]$$

The unknowns,  $z$  &  $n$ , are determined by inserting the appropriate values of  $x$  and simultaneously solving equations (3) & (6).

The determination of the depth ( $z$ ) is important but  $n$  as a measure of the rate of fall-off is also of interest as it adds to the knowledge of the extent or shape of the mass causing the anomaly. This information may aid in the separation of anomalies that owe their origin to differentiations within the basement from those that are caused by structural deformation of the basement.

Many methods are possible utilizing the various derivations of Euler's Theorem, The derivative with respect to  $z$  is

$$(7) \quad \frac{\partial^2 H}{\partial x \partial z} x + \frac{\partial^2 H}{\partial y \partial z} y + \frac{\partial^2 H}{\partial z^2} z + \frac{\partial H}{\partial z} = n \frac{\partial H}{\partial z}$$

When this equation is evaluated at the peak of the first derivative map

$$\frac{\partial^2 H}{\partial x \partial z} = \frac{\partial \left( \frac{\partial H}{\partial z} \right)}{\partial x} = 0$$

$$\frac{\partial^2 H}{\partial y \partial z} = \frac{\partial \left( \frac{\partial H}{\partial z} \right)}{\partial y} = 0$$

and the simplified Euler's Vertical Derivative Theorem becomes

$$(8) \quad \frac{\partial^2 H}{\partial z^2} \Big|_2 \cdot z = (n - 1) \frac{\partial H}{\partial z} \Big|_2$$

Solving for  $z$  with equation (3),

$$(9) \quad z = \frac{\frac{\partial H}{\partial z} \Big|_2}{\frac{1}{H_1} \frac{\partial H}{\partial z} \Big|_1 - \frac{\partial H}{\partial z} \Big|_2 - \frac{\partial^2 H}{\partial z^2} \Big|_2}$$

Here, too, difference methods can be employed to overcome the difficulty of determining the absolute values of the field and its derivatives. It is important to note that in all methods described herein errors in determining  $z$  depend largely upon the accuracy of the computed derivative maps (if one obtains the derivatives by computational methods applied to a magnetic field map), its contours, and the individual's interpolation.

The horizontal derivative of Euler's Theorem can be pressed as

$$(10) \quad \frac{\partial^2 H}{\partial x^2} x + \frac{\partial^2 H}{\partial y \partial x} y + \frac{\partial^2 H}{\partial z \partial x} z = (n-1) \frac{\partial H}{\partial x}$$

Given a total intensity anomaly profile, which again is perpendicular to the contour lines

$$\frac{\partial^2 H}{\partial y \partial x} = 0$$

where the profile is in the x-direction. In this region of

$$\frac{\partial^2 H}{\partial y \partial x} = 0 \quad \text{and at the inflection point of the profile, clearly}$$

$$\frac{\partial^2 H}{\partial x^2} = 0$$

Thus,

$$(11) \quad z = (n-1) \frac{\frac{\partial H}{\partial x}}{\frac{\partial^2 H}{\partial z \partial x}}$$

This method is used in addition to the other derivations of  $z = f(n)$  largely because it is not dependent upon the knowledge of the absolute values of the field or the gradient but only upon their slopes.

Of some interest is an approach to equation (11) based not upon Euler's Theorem but upon an application of scalar (dot)

product of two pertinent quantities: the gradient of the scalar  $H$  and the radius vector from the source to the point of observation.

The quantity measured by the magnetometer, as previously mentioned, is simply the intensity of the earth's total field vector, a scalar quantity. The gradient of this scalar field is

$$\vec{\nabla} H = \vec{i} \frac{\partial H}{\partial x} + \vec{j} \frac{\partial H}{\partial y} + \vec{k} \frac{\partial H}{\partial z}$$

$$|\vec{\nabla} H| = \sqrt{\left(\frac{\partial H}{\partial x}\right)^2 + \left(\frac{\partial H}{\partial y}\right)^2 + \left(\frac{\partial H}{\partial z}\right)^2}$$

The scalar product of the gradient and the radius vector is

$$(12) \quad \vec{r} \cdot \vec{\nabla} H = \frac{\partial H}{\partial x} x + \frac{\partial H}{\partial y} y + \frac{\partial H}{\partial z} z = |\vec{\nabla} H| |\vec{r}| \cos \theta$$

$$\text{where } \vec{r} = \vec{i} x + \vec{j} y + \vec{k} z$$

$$\text{and } |\vec{r}| = \sqrt{x^2 + y^2 + z^2}$$

$$\text{and } \theta = \text{angle between } \vec{\nabla} H \text{ and } \vec{r}.$$

The derivative with respect to  $x$  of the scalar product is

$$(13) \quad \frac{\partial (\vec{r} \cdot \vec{\nabla} H)}{\partial x} = \frac{\partial^2 H}{\partial x^2} x + \frac{\partial H}{\partial x} + \frac{\partial^2 H}{\partial y \partial x} y + \frac{\partial^2 H}{\partial z \partial x} z = \frac{\partial (|\vec{r}| |\vec{\nabla} H| \cos \theta)}{\partial x}$$

If the same conditions are applied to this equation as were imposed upon equation (10), then equation (13) reduces to

$$(14) \quad z = \frac{\frac{\partial(|\vec{r}| |\nabla H| \cos \theta)}{\partial x} - \frac{\partial H}{\partial x}}{\frac{\partial^2 H}{\partial z \partial x}}$$

which is an implicit function of  $z$  and can be solved as follows:

The first term on the right hand side of the equation contains a function of  $z$  in the factor,  $|\vec{r}| \cos \theta$ . By evaluating the slope of the scalar product versus  $x$  for assumed values of  $z$  and inserting the values of this term in equation (14), one value of  $z$  will be identical with the assumed  $z$ . This represents a graphical solution for the implicit function of the unknown depth,  $z$ .

This last method of solving for the depth,  $z$ , is advantageous in that one has only a single unknown, that the measured parameters are independent of the knowledge of the absolute value of the anomaly, and that the equation does not require the field,  $H$ , to be mathematically homogeneous. It can be shown that Euler's Theorem is a special case of the scalar product equation in which  $H$  is a homogeneous function.

## 2. A Model Study Demonstrating Euler's Theorem as Applied to Basement Depth Determinations.

In order to test theories on depth determination using gradient and total field data, simple model tests were performed on the evening of September 22, 1961 on the magnetometer test pad of Varian Associates. The results of the tests confirmed various theories directly applicable to the problem of determination of depth to basement from derivative information.

The methods proposed for the computation of depth involves the knowledge of the total magnetic field and the vertical gradient on a profile directly over the peak of the total field contours. The source is the origin ( $x=y=z=0$ ), the  $z$ -axis is vertical and positive upwards, and  $y$  is the third member of a positive orthogonal triple.

As a matter of practical convenience the whole coordinate system was rotated  $90^\circ$  about the  $x$  axis so that  $z$  was then in a horizontal plane and approximately  $15^\circ$  east of magnetic north. The study was designed to be two dimensional so that both the point of observation and the gradient were approximately zero in the  $y$  direction. Also it was found to be more convenient to move the source relative to the instruments as opposed to the case in practice where the instruments move relative to the source and the environment. Assuming the environment to be homogeneous as compared to the magnitude of the source, the same end would be achieved in either case.

The axis of the gradiometer was horizontal and approximately five feet above the flat black-top surface of the parking lot adjacent to the test pad. Parallel lines were drawn perpendicular to the z axis at distances of 45, 50, 55, 60, and 65 feet from the center of the gradiometer. The gradiometer itself consisted of two magnetometers five feet apart whose signals were beat together to obtain the difference between them. See Figure 11. One of them was used as a magnetometer and the data corrected two and a half feet to the center of the gradiometer system using the value of the gradient and observed value of the total magnetic field.

The source used was a large permanent bar magnet approximately eight inches long. On the runs where the signal to the gradiometer was weak, two such magnets were aligned end to end and used as the source. The magnet was taped to a three foot wooden pole and the pole, in turn, rested on a line drawn on a non-magnetic cart about three feet high.

The cart was pulled by hand at about one foot per second along the traverse lines and timing marks placed on the records every ten feet from  $x = -130$  to  $x = +130$ . Radio communication was used throughout the test to insure the correct logging of events. See Figures 12, 13.

The main purpose of the tests was to verify the correctness of Euler's Theorem as used in depth determination.

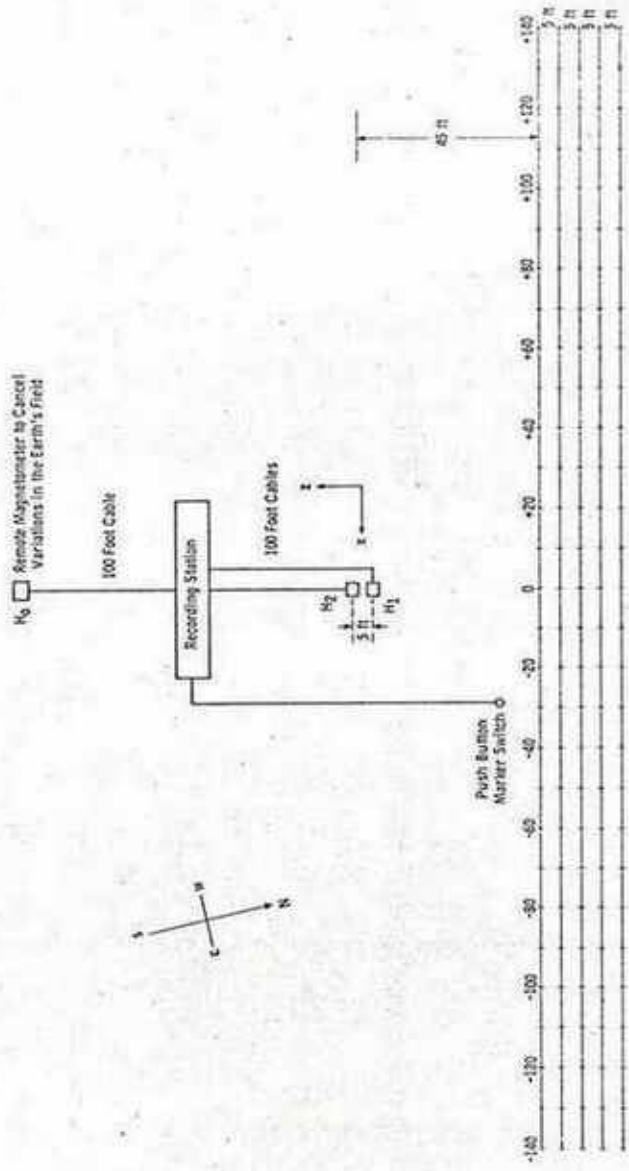


**FIGURE 11.**  
**THE EXPERIMENTAL SETUP USED FOR THE MODEL TESTS. A PERMANENT BAR MAGNET**  
**SIMULATING A MAGNETIC DEPOSIT WAS MOVED ALONG**  
**EACH PROFILE ON A NONMAGNETIC CART.**

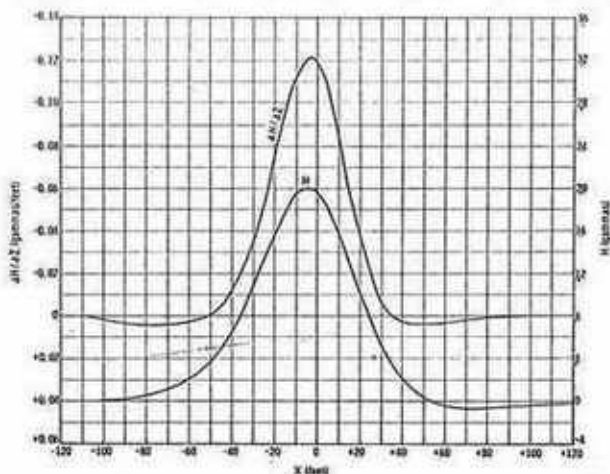


**FIGURE 12.**  
**GRADIOMETER ANOMALY AND CORRECTED MAGNETOMETER**  
**ANOMALY OBTAINED FOR A BAR MAGNET PASSING**  
**BY AT A DISTANCE OF 50 FEET**

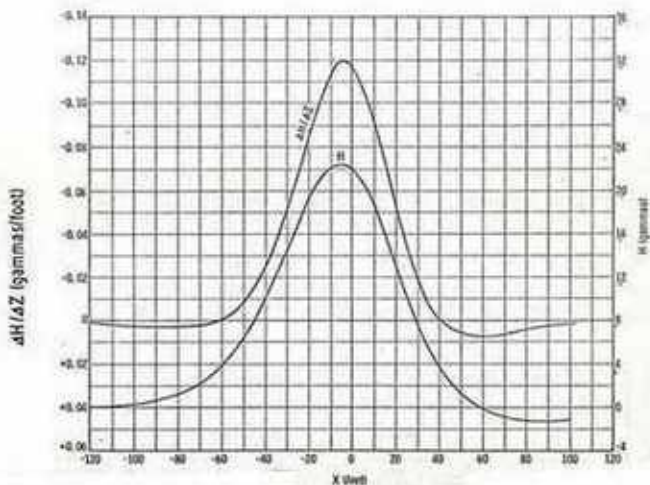


**FIGURE 13.**  
**GRADIOMETER ANOMALY AND CORRECTED MAGNETOMETER**  
**ANOMALY OBTAINED FOR A LARGE BAR MAGNET PASSING BY**  
**AT A DISTANCE OF 60 FEET**

In the situation that exists in the model tests both  $y$  and  $\frac{\partial H}{\partial y}$  are essentially zero and we have for the 'depth'  $z$ ,

$$z = \frac{n H - x \frac{\partial H}{\partial x}}{\frac{\partial H}{\partial z}}$$

and  $\frac{\partial H}{\partial z}$  is the value of the gradient at the gradiometer

$H$  &  $\frac{\partial H}{\partial x}$  are obtained from the total field profile,

and  $x$  is known from the method described in II, 1.

Solving for  $z$  and  $n$  by using simultaneous equations,

$$z = n \frac{H|_{\text{peak}}}{\frac{\partial H}{\partial z} |_{\text{peak}}} \quad \text{at the peak of the total field profile where } x = 0,$$

and 
$$z = \frac{n H_1 - x \frac{\partial H}{\partial x} |_1}{\frac{\partial H}{\partial z} |_1}$$

The determination of  $z$  and  $n$  are graphically represented in Figures 14, 15.

The profiles were added according to the law of super-

position to obtain a summation curve of  $H$  and  $\frac{\partial H}{\partial z}$  for a configuration of magnets at  $z = 45, 50, 55, 60,$  and  $65$  feet and displaced by  $0, 10,$  and  $20$  feet either side of the original position. The center of this configuration is approximately  $55$  feet.

By scalar product method

$$x \frac{\partial^2 H}{\partial x^2} + \frac{\partial H}{\partial x} + y \frac{\partial^2 H}{\partial y \partial x} + z \frac{\partial^2 H}{\partial z \partial x} = \frac{\partial(|\vec{\nabla} H| |\vec{r}| \cos \theta)}{\partial x}$$

$$z = \frac{\frac{\partial(|\vec{\nabla} H| |\vec{r}| \cos \theta)}{\partial x} - \frac{\partial H}{\partial x}}{\frac{\partial^2 H}{\partial z \partial x}} \quad \text{where } |\vec{r}| = \sqrt{x^2 + z^2}$$

Applied to the summation curves,

$z = 50$  feet and  $58$  feet for the west and east side of the profiles respectively. Euler's Theorem appeared to produce inconsistent results for various values of  $x$  explained in part by the degree of inhomogeneity of the relatively large size (array) of the source.

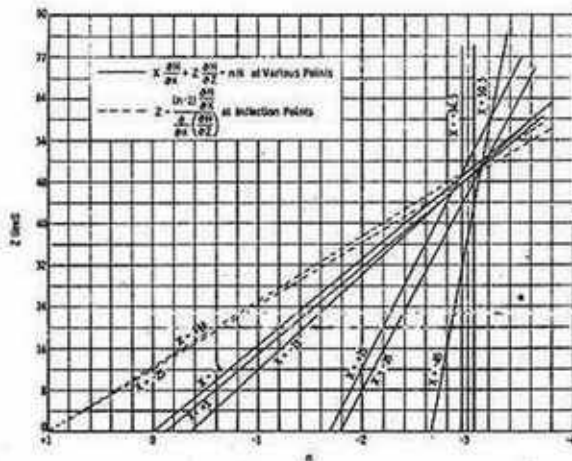


FIGURE 14.  
SOLUTION FOR Z AND n OBTAINED FROM THE MODEL RESULTS  
OF FIGURE 3 FOR A PERMANENT MAGNET DIPOLE AT 50 FEET

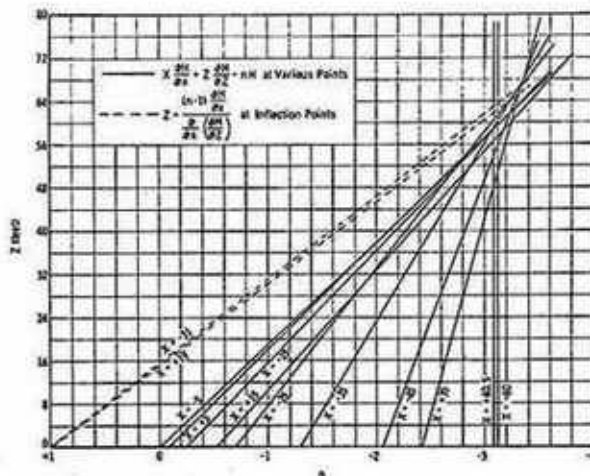


FIGURE 15.  
SOLUTION FOR Z AND n OBTAINED FROM THE MODEL  
RESULTS OF FIGURE 4 FOR A PERMANENT MAGNET DIPOLE AT 60 FEET

## Part IV

### Conclusions

The introduction of objective derivative calculations has effectively provided the additional equation necessary to solve for the geophysically important unknowns of basement topography, such as depth to basement and type of basement disturbance. The gradiometer may bridge the gap between the low resolution of air surveys and the high resolution of the seismograph.

The great advances in instrumentation that enabled one to measure changes of intensity to one in 100,000 has not stimulated a proportional advancement in interpretation of magnetic surveys. For all practical purposes interpretation remains either completely qualitative; quasi-quantitative and based upon empirical studies; or approximately quantitative where the shape, size, and susceptibility of a body are assumed and calculations based upon these.

Assuming good control on a given aeromagnetic map, it appears that H contains more potential information than is presently utilized by geophysical interpreters, particularly in the realm of derivatives. The ability to detect changes in the field to one part in ten million is now realized; computers have made possible field calculations previously thought to be prohibitive; and future automatic recording and plotting methods may short circuit the error-producing, laborious contouring methods that now limit methods based upon field theory.

## Acknowledgments

The work was undertaken as a student of Professor Joshua L. Soske, Department of Geophysics, Stanford University. Experience and curiosity gained from his in and out of the classroom discussions generated the desire to "find a better way to do it." It is a pleasure to thank him for a highly cherished education and friendship.

Originally the research was oriented towards a method of measurement and theory of interpretation of the second derivative. Heading toward this goal, the writer was employed by Varian Associates of Palo Alto, California. This work was carried out in their employ under contract to the Pure Oil Company, Palatine, Illinois. Many thanks go to these firms and to Mr. Ken Ruddock for his criticism and very capable engineering on this instruments and to Dr. Howard A. Slack with whom much of this investigation was performed.

## Appendix

The application of Euler's Theorem requires the determination of the derivative of the field value in the  $z$  direction; that is  $\frac{\partial H}{\partial z}$ . The method is to approximate this derivative value by measuring the difference in the magnetic field  $\Delta H$  at two points separated by a finite distance  $\Delta z$ , and taking  $\frac{\Delta H}{\Delta z}$  as the derivative. When  $\Delta z$  is very small compared to the distance from the magnetic source this is obviously a good approximation. In the model work however  $\Delta z$  is of the order of one-tenth of the distance from the source. It is necessary to establish the magnitude of the error in setting  $\frac{\Delta H}{\Delta z} = \frac{\partial H}{\partial z}$  at the midpoint of  $\Delta z$ .



A simple case along the  $z$  axis is considered. The source is a dipole of magnetic moment  $K$  along the  $z$  axis. Then at any point along the  $z$  axis

$$H = \frac{K}{z^3} \quad \text{and} \quad \frac{\partial H}{\partial z} = -3 \frac{K}{z^4}$$

The field at a point  $(z - .05 z)$  is  $H_1 = \frac{K}{(z - .05 z)^3}$  and at a

point  $(z + .05 z)$  is  $H_2 = \frac{K}{(z + .05 z)^3}$

$$H_1 = \frac{K}{z^3(1 - .05)^3} = \frac{K}{0.8574 z^3} = 1.1663 \frac{K}{z^3}$$

$$H_2 = \frac{K}{z^3(1+.05)^3} = 1.1576 z^3 = 0.8637 \frac{K}{z^3}$$

$$\Delta H = H_2 - H_1 = (0.8637 - 1.1663) \frac{K}{z^3} = -0.3026 \frac{K}{z^3}$$

$$\Delta z = 0.10 z$$

$$\frac{\Delta H}{\Delta z} = \frac{-0.3026 \frac{K}{z^3}}{0.10 z} = -\frac{3.026 \frac{K}{z^3}}{z^4}$$

Error in use of  $\frac{\Delta H}{\Delta z}$  for  $\frac{\partial H}{\partial z} = \frac{\frac{\Delta H}{\Delta z}}{\frac{\partial H}{\partial z}} = \frac{-3.026}{-3.0} = 1.009$  or less

than 1 per cent for  $z \leq 0.10 z$ .

The above shows that a sufficiently good value can be obtained at the point midway between the two magnetometer heads. To obtain the value of H at this same point it is proposed to use  $H = H_2 - \frac{\Delta H}{2}$ . It is necessary to establish the magnitude of the error in this approximation.

$$H_2 = 0.8637 \frac{K}{z^3}$$

$$\Delta H = -0.3026 \frac{K}{z^3} \quad \text{from above}$$

$$H_2 - \frac{\Delta H}{2} = (0.8637 + 0.1513) \frac{K}{z^3} = 1.015 \frac{K}{z^3}$$

But  $H = \frac{K}{z^3}$  so the error in the use of  $H_2 - \frac{\Delta H}{2}$  for H is

$$\frac{H_2 - \frac{\Delta H}{2}}{H} = \frac{1.015}{1} = 1.015 \quad \text{or } \leq 1 \frac{1}{2} \text{ per cent for } z \leq 0.10 z$$

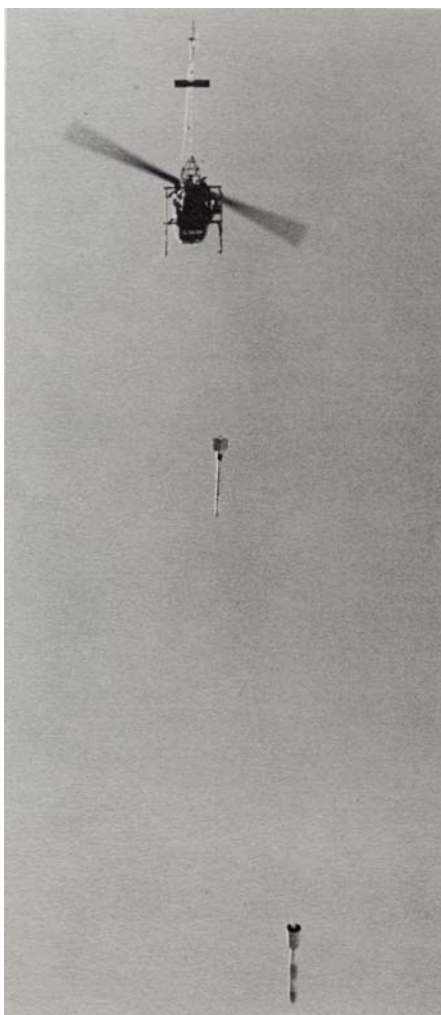
This is sufficiently good for the purpose of the model tests.

## REFERENCES

- Baranov, V., 1953, Calcul du gradient vertical duc hamp de gravité ou du champ magnetique mesure a la surface du sol: Geophysical Prospecting, v.1, p. 171-191.
- Bullerwell, W., 1961, Interpretation of Geophysical Surveys: Nature, v.192, p. 1242-1244.
- Dean, W.C., 1958, Frequency analysis for gravity and magnetic interpretation: Geophysics, v.23, p.97-127.
- Dobrin, M.B., 1952, Introduction to geophysical prospecting: New York, McGraw-Hill Book Company, Inc.
- Elkins, T.A., 1951, The second derivative method of gravity interpretation: Geophysics, v.16, p.29-50.
- Evjen, H.M., 1936, The place of the vertical gradient in gravity interpretation: Geophysics, v.1, p.127-136.
- Grant, F.S., 1952, Three dimensional interpretation of gravity anomalies, Part II: Geophysics, v.17, no.4, p.756-789.
- Griffin, W.R., 1949, Residual gravity in theory and practice: Geophysics, v.14, no.1, p.39-56.
- Hammer, S., 1950, Recent developments in gravity prospecting: Colo. School of Mines Quarterly, v.45, no.4A, p.87-103.
- Henderson, R.G., 1960, A Comprehensive system of automatic computation in magnetic and gravity interpretation: Geophysics, v.25, no.3, p.569-585.
- Henderson, R.G., Zietz, I., Computation of second vertical derivatives of geomagnetic fields: Geophysics, v.14, no.4, p.508-535, 1949.
- \_\_\_\_\_, 1949, Upward continuation of anomalies in total magnetic intensity fields: Geophysics, v.14, no.4, p.517-535.
- \_\_\_\_\_, 1955, The sudbury aeromagnetic map as a test of interpretation method: Geophysics, v.20, No. 2, p. 307-317.
- Kogbetliantz, E.R., 1944, Quantitative interpretation of magnetic and gravitational anomalies: Geophysics, v.9, p.463-493.
- Nettleton, L.L., Regionals, residuals, and structures: Geophysics, v.19, no.1, p.1-22, 1954.
- Peters, L.J., 1949, The direct approach to magnetic interpretation and its practical application: Geophysics, v.14, p.290-320.
- Rosenbach, O., 1954, Quantitative studies concerning the vertical gradient and second derivative methods of gravity interpretation: Geophysical Prospecting, v.2, p.128-138.
- Skeels, D.C. and Watson, R.J., 1949, Derivation of magnetic and gravitational quantities by surface integration: Geophysics, v.14, p.133-150.
- Trejo, C.A., 1954, A note on downward continuation of gravity: Geophysics, v.19, p.71-75.
- Vacquier, V, et al, Interpretation of aeromagnetic maps: Geological Society of America, memoir no. 47, 1951.

# Airborne Magnetic Gradiometer for Petroleum Exploration

(Invented by Sheldon Breiner in 1961, as part of a research project for his M.S. Geophysics at Stanford University. Patent assigned to Varian Associates.)



A new geophysical prospecting device, developed by the Quantum Electronics Division of Varian, is now in use by a major oil company to map the earth's subterranean geology. The device, known as an airborne geomagnetic gradiometer, provides outlines of the shape, size, and depth of underground formations indicative of oil deposits.

The new airborne system, which consists of two Varian rubidium magnetometers, can map several hundred miles of terrain per day to provide geologists with detailed data on which to base seismic analyses on the ground. The Quantum Electronics Division (QED) has received a \$500,000 contract for the new geomagnetic instruments, which have been under field evaluation for five years. The Union Oil Company of California is Varian's licensee for airborne geomagnetic surveys.

## Gradiometer Description

The airborne gradiometer, its concept and principles were conceived by Dr. Sheldon Breiner as his Master of Science research project in Geophysics at Stanford University. He applied for and received a patent, assigned to Varian Associates as a condition of his borrowing two rubidium magnetometer sensors to carry out his work. The vertical optically-pumped magnetic gradiometer consists of two rubidium

magnetometers housed in separate aerodynamic pods suspended with 100 feet of vertical separation beneath a helicopter or airplane (but no horizontal separation, after correction for airspeed). Each capable of sensing a change in the earth's magnetic field of 0.01 gamma [now, 0.01 nanoTesla, or 10 picoTesla], a sensitivity equal to one part in five million of the earth's total magnetic field. The output of the lower magnetometer and the difference between the two is recorded simultaneously by instrumentation within the aircraft.

## Advantages of the Magnetic Gradiometer

Whereas previous aeromagnetic studies using a magnetometer proved adequate in charting the total or regional magnetic fields, the gradiometer, by using two sensors, offers the petroleum geologist several significant advantages:

First of course, is the vertical measurement sensitivity. This enables the geologist to determine the depth and characteristics of underlying or basement structures and their probable effect on the overlying sedimentary strata in which oil is found.

Another previous stumbling block to highly accurate aerial geomagnetic prospecting was the continual change over time in intensity of the earth's magnetic field itself. The dual sensor configuration of the gradiometer automatically eliminates such changes and prevents the consequential distortion of the magnetic measurements.

The end result of the actual field survey consists of a map of the total magnetic field and a map of the vertical gradient of the field--both of which are synchronized to the position of the aircraft. To the petroleum professional, this presents a picture of the nature and configuration of the subsurface rocks which might contain petroleum.

### **Euler's Equation**

A key attribute and the basic impetus for the gradiometer was Breiner's innovation in the April, 1961 whereby he used the three components of the gradient and the magnitude of the total magnetic field of the earth to compute the distance between the magnetometer sensors (actually, the midpoint between them) and the upper surface of the magnetic (crystalline) basement rocks which underlie all petroleum basins. The mathematical relationship between these magnetic field attributes is described by what is known as Euler's theorem on homogeneous functions. A constant, called, "n" in the equation (also the rate of 'fall-off' of the magnetic field of the anomaly source) is an important descriptive parameter which characterizes the physical nature of the magnetic source, be it a semi-infinite block, a dike, anticline, a volcanic plug or a dipolar source, all of whose dimensions are small relative to the distance between the gradiometer sensors and the source minerals, namely, magnetite.

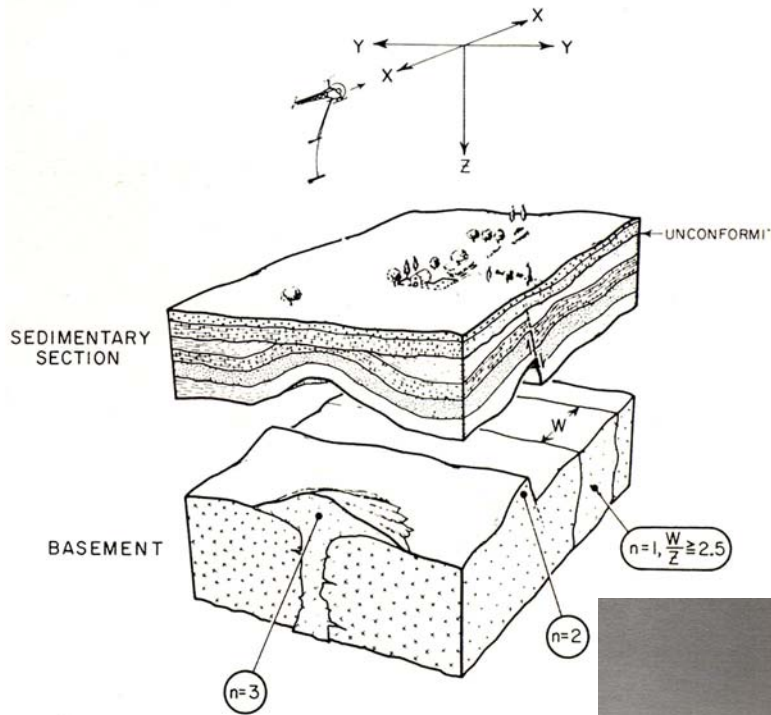
According to Varian, the tens of thousands of field survey miles flown have indicated the gradiometer will provide a profitable shortcut in preliminary prospecting stages over much of the earth's surface.

The rubidium magnetometers comprising the Varian gradiometer have been under development and refinement by the Quantum Electronics Division since 1957, licensed from the inventor of optically-pumped alkali-vapor magnetometer, Professor Hans Dehmelt of the University of Washington and subsequently a Nobel Laureate.



Breiner near Monument Valley, Arizona, testing the first rubidium airborne magnetic gradiometer, October, 1961

DIAGRAMMATIC CROSS-SECTION AND  
SIGNIFICANCE OF THE "n" AS IT RELATES TO  
THE CHARACTERISTICS OF THE GEOLOGY



# Magnetic Airborne Magnetic Gradiometer Patent

## 1. US PATENT REFERENCE:

TITLE: METHOD FOR DETERMINING DEPTH AND  
FALLOFF RATE OF  
SUBTERRANEAN MAGNETIC  
DISTURBANCES UTILIZING A  
PLURALITY OF MAGNETOMETERS  
INVENTOR(S): **BREINER SHELDON**; RUDDOCK KENNETH  
A; SLACK, HOWARD A  
PATENT ASSIGNEE(S): PURE OIL CO THE (68744)  
VARIAN ASSOCIATES INC (88480)

	NUMBER	DATE
PATENT INFORMATION:	US 3263161	19660726
	(CITED IN 010 LATER PATENTS)	
EXPIRATION DATE:	26 Jul 1983	
FAMILY INFORMATION:	US 3263161	19660726
DOCUMENT TYPE:	UTILITY; REASSIGNED	

THE METHOD OF DETERMINING THE DEPTH Z AND FALL-OFF  
RATE N OF A  
SUBTERRANEAN MAGNETIC DISTURBANCE BELOW AN AREA TO BE  
SURVEYED,  
COMPRISING: DETERMINING THE MAGNETIC INTENSITY H AND  
THE VERTICAL  
GRADIENT  $\frac{\partial H}{\partial Z}$  OF THE EARTH'S MAGNETIC FIELD FOR AT  
LEAST TWO POINTS OF  
SUBSTANTIALLY CONSTANT ELEVATION LYING WITHIN THE  
AREA TO BE SURVEYED;  
LOCATING THE HORIZONTAL COORDINATES X, Y OF SAID  
POINTS WITH RESPECT TO  
THE CENTER OF SAID SUBTERRANEAN DISTURBANCE;  
CONSTRUCTING AT LEAST ONE  
PROFILE OF THE TOTAL FIELD H; DETERMINING THE  
HORIZONTAL SPACE  
DERIVATIVES  $\frac{\partial H}{\partial X}$ ,  $\frac{\partial H}{\partial Y}$  FROM THE SLOPE OF SAID  
PROFILE AT SAID